Biomaterials 35 (2014) 3736–3743

Contents lists available at ScienceDirect

Biomaterials

journal homepage: www.elsevier.com/locate/biomaterials

A tunable silk–alginate hydrogel scaffold for stem cell culture and transplantation

Keren Ziv [a,1], Harald Nuhn [b,1], Yael Ben-Haim [a], Laura S. Sasportas [a,b], Paul J. Kempen [c], Thomas P. Niedringhaus [b], Michael Hrynyk [d], Robert Sinclair [c], Annelise E. Barron [b], Sanjiv S. Gambhir [a,b,c,*]

[a] Molecular Imaging Program at Stanford (MIPS), Department of Radiology, CA, USA
[b] Department of Bioengineering, Stanford University, CA, USA
[c] Department of Materials Science and Engineering, Stanford University, CA, USA
[d] Department of Chemical Engineering, Queen's University, Ontario, Canada

ARTICLE INFO

Article history:
Received 30 December 2013
Accepted 10 January 2014
Available online 28 January 2014

Keywords:
Silk
Alginate
Laminin
Scaffold
Stem cells
Elasticity

ABSTRACT

One of the major challenges in regenerative medicine is the ability to recreate the stem cell niche, which is defined by its signaling molecules, the creation of cytokine gradients, and the modulation of matrix stiffness. A wide range of scaffolds has been developed in order to recapitulate the stem cell niche, among them hydrogels. This paper reports the development of a new silk–alginate based hydrogel with a focus on stem cell culture. This biocomposite allows to fine tune its elasticity during cell culture, addressing the importance of mechanotransduction during stem cell differentiation. The silk–alginate scaffold promotes adherence of mouse embryonic stem cells and cell survival upon transplantation. In addition, it has tunable stiffness as function of the silk–alginate ratio and the concentration of crosslinker – a characteristic that is very hard to accomplish in current hydrogels.

The hydrogel and the presented results represents key steps on the way of creating artificial stem cell niche, opening up new paths in regenerative medicine.

1. Introduction

Stem cell therapy is a powerful therapeutic intervention that has the potential to combat several autoimmune, cancer and metabolic diseases [1–3]. Unfortunately, due to the rarity and fragility of progenitor cell populations, limited ex-vivo growth potential, few successful stem cell culture systems, and poor integration into host tissues upon transplantation, the widespread use of stem cell therapies in the clinic is limited [4,5].

The primary obstacle in developing stem cell based therapies subsequently, lies within the ability to recreate the microenvironment in which stem cells naturally reside in. *In vivo*, the stem cells live within a niche, which is described as a highly specialized microenvironment. This milieu integrates both established supportive cells, as well as a complex extracellular matrix (ECM) consisting of a network of proteins, such as collagens, or elastin arranged in a three-dimensional network. The orientation, elasticity and fluid handling properties of these network fibers help to dictate the biomechanical properties of the niche. In addition, these properties of the microenvironment determine the stem cell fate (i.e., self-renewal vs. differentiation) through a number of different, complementary mechanisms, including the well-defined presentation of various signaling molecules, the creation of cytokine gradients, and the modulation of matrix stiffness [6–8].

The microenvironment plays a pivotal role in determining cell identity and behavior by providing a suitable niche to sustain self-renewal and differentiation capacity [6,7,9]. Therefore, mimicking the stem cell niche, (i.e., preparing an artificial niche), is key to facilitating in vitro expansion of freshly isolated stem cells pre- or post-transplantation [8,10].

Current approaches to prepare a suitable environment that supports stem cell survival and differentiation, are based upon mimicking the host environment to the stem cell niche as much as possible [11]. For this purpose, scaffolds have been prepared using biopolymers and other molecules found in the ECM, such as

* Corresponding author. Molecular Imaging Program at Stanford (MIPS), Radiology Department, E150 James Clark Center, 318 Campus Drive, Stanford, CA 94305, USA. Tel.: +1 650 725 2309; fax: +1 650 724 4948.
E-mail address: sgambhir@stanford.edu (S.S. Gambhir).
[1] Equal contribution.

0142-9612/$ – see front matter © 2014 Elsevier Ltd. All rights reserved.
http://dx.doi.org/10.1016/j.biomaterials.2014.01.029

collagen, elastin [12], fibrinogen, fibrin, hyaluronic acid, glycosaminoglycans (GAGs), hydroxyapatite, Matrigel, silk, alginate or chitosan to accomplish this goal [12–19]. These polymers have the advantage of being bioactive.

Besides natural polymers, synthetic polymers are widely used to form scaffolds for stem cell cultivation [20]. The most prominent examples include poly(ethylene glycol) (PEG) and acrylated hydrogels [14]. Among the synthetic class of polymers, are biodegradable ones such as, polyglycolic acid (PGA), polylactic acid (PLA), poly(ε-caprolactone) (PCL) and the copolymer poly(lactic-co-glycolic acid) (PLGA). These synthetic polymers have been used extensively as synthetic 3D scaffold materials for evaluating cell behavior, however, fail in recreating the same biomechanical properties and structural complexity found naturally in the ECM.

Different studies show that stem cell survival and phenotype can be controlled by attenuating the mechanical properties of biosynthetic matrices [8,9,15,21]. Gaining the ability to generate and control the mechanical properties of stem cell scaffolds is therefore very important and practical in developing stem cell based therapies. In this proof of concept study we address the need for simulating the mechanical and structural properties of the niche. We report on the preparation and characterization of a newly designed silk–alginate based hydrogel, of defined molecular composition and topology that addresses the unmet need for a mechanically adjustable scaffold to support and with the potential to guide stem cell survival and differentiation, respectively. The combination of these two very different types of biomaterials, silk and alginate, results in a hybrid class of rapidly gelling, physically stable hydrogels overcoming the biomechanical limitations of current hydrogels for several applications in regenerative and pharmaceutical applications, such as 3D printed organs, or organs-on-a-chip as e.g. drug screening platform [22].

2. Materials and methods

2.1. Scaffold formation

Hydrogel precursor mixtures were prepared from alginate 4w/v% in distilled water (Protanal® LFR 5/60 Sodium Alginate with high alpha-L-guluronate (G) residues kindly provided by FMC Biopolymers, Ewing, NJ) and 7.4 – 7.8 w/v% silk solution in distilled water (freshly prepared *Bombyx mori* silkworm silk solutions kindly provided by Prof. David Kaplan, Tufts University, Boston, MA). Precursor mixtures were supplemented by one of the following: 0.5 mg/mL mouse laminin (Roche, Indianapolis, IN), 0.5 mg/mL fibronectin (Roche, Indianapolis), 1 mg/mL in pH 6.5 in BIS–TRIS (10 mM) Bovine collagen I (MP Biomedicals, Santa Ana, CA), or 0.5 mg/mL cyclic RGD (Peptides International, Louisville, KY). Concentrations of the final precursor solutions were adjusted using distilled water to reach a final concentration of 1.5% w/w silk and 1% w/w alginate. Precursor mixtures were mixed until they appeared homogeneous. For all experiments the bubble-free precursor solution was injected into a custom mold, enabling the simultaneous preparation of 6 disc-shaped hydrogel samples (8 mm diameter, 1.56 mm thickness). The mold was covered on both sides by a dialysis membrane (50,000 MWCO, Spectrum Laboratories, Houston, Tx), allowing calcium ions to enter and induce gelation. Following injection of the precursor solution into the mold, gelation was induced by immersing the mold in a buffered 25 mM $CaCl_2$ solution (Sigma Aldrich) (10 mM BIS–TRIS, 100 mM NaCl, pH 6.5, Sigma–Aldrich, USA, and Anachemia, Reno, NV, respectively). Gelation time ranged from 20 to 60 min. Scaffolds for cell adherence experiments were cast in 12-well transwell plates (Corning, Lowell, MA) using the same precursor solutions and gelation conditions described above.

2.2. Cell culture and bioluminescence imaging

Following casting of the different hydrogel precursor mixtures in 12-well transwell plates, D3 mouse embryonic stem cells (mESC) expressing firefly luciferase (Fluc) were plated (200,000 cells/well) and cultured with the appropriate medium (D3 mESCs were cultured on gelatin-coated 10 cm dishes with knock-out Dulbecco's modified Eagle's medium (D-MEM) (GIBCO/BRL, Grand Island, NY, USA), containing 15% knock-out fetal bovine serum (FBS) (Invitrogen, Grand Island, NY, USA), 1% nonessential amino acids (GIBCO/BRL), 0.1 mmol/L 2-mercaptoethanol (GIBCO/BRL), 1000 U/mL mouse recombinant leukemia inhibitory factor (LIF) (GIBCO/BRL), 100 IU/mL penicillin, and 0.1 mg/mL streptomycin). 72 h after plating, the cells were tested for Fluc expression as an indicator for cell presence and viability using bioluminescence imaging (BLI). The luciferase substrate, D-Luciferin (BIOSYNTH, Itasca, IL), was added to each well (2 μg/mL). Cells were imaged immediately after the addition of substrate using an IVIS-200 imaging system equipped with a cooled charge-coupled device camera (Caliper). Imaging was performed using open filters. Regions of interest were drawn over each well, and the average radiance was determined using Living Image software (V4.1, Caliper Life Sciences).

2.3. Window chamber implantation

All animal handling was performed in accordance with Stanford University's Animal Research Committee guidelines.

A dorsal skinfold window chamber was surgically implanted in female Balb/C mice (Charles River, 10 weeks of age). Animals were anesthetized by intraperitorneal (IP) injection of a mixture of 1 mg/mL of xylazine and 10 mg/mL ketamine in 300 μL final volume. Hair was removed from the mice's backs using hair clippers and depilatory cream (Nair, naircare.com). Next, medium-sized titanium dorsal skinfold window chambers (APJ Trading, Cat.# MD100) were surgically implanted on the back of the animals, as previously described [23]. Briefly, following the midline, a titanium frame was sutured to the dorsal side using surgical sutures (Blue Polypropylene, 5-0, FS-2) (Med Rep Express, Patricia Brafford, MA). Both layers of the skin flap were punctured in two instances to secure two stainless steel screws. A round-shaped epidermal layer was removed from the upward-facing skin flap and covered by a sterile 12 mm diameter glass coverslip. Following this, both frames were screwed together and sutured to the skin flap. The animals were allowed to recover over a period of 3–4 days, after which the scaffold was implanted. For the implantation, the coverslip was removed using pliers, followed by placement of the scaffold onto the dermal layer inside the window chamber and covering with a fresh coverslip.

2.4. Fluorescent alginate synthesis

For the purpose of window chamber intravital microscopy (IVM) experiments, we transplanted fluorescent scaffolds, in which the alginate (Sigma–Aldrich, USA) was labeled with rhodamine B isothiocyanate (RBITC) (Sigma Aldrich, Milwaukee, WI). Alginate was labeled with RBITC according to a method previously reported by Mladenovska et al. [24]. Briefly, an aqueous 2w/w% alginate solution was prepared and adjusted to a pH = 8 by adding 1 M sodium hydroxide (Anachemia, Reno, NV). An RBITC solution was prepared by mixing 1 mg of RBITC in 1 mL DMSO (Fisher, Fairlawn, NJ) followed by slow addition into the alginate solution. The alginate–RBITC mixture was stirred for 1 h at 40 °C. After stirring, 0.5349 g of NH_4Cl (Sigma Aldrich) was added and mixed until fully dissolved. The alginate–RBITC solution was dialyzed in darkness overnight. Water baths were frequently changed with distilled deionized water. Subsequently, the alginate–RBITC solution was poured into 50 mL polypropylene conical vials until approximately three-quarters full, flash frozen at −80 °C and lyophilized until fully dry. Lyophilized alginate–RBITC was stored at −20 °C until use.

2.5. Intravital microscopy (IVM)

Fluorescent scaffolds were transplanted in mice with a dorsal skinfold window chamber (n = 4). Intravital Microscopy (IVM) was used to track the scaffold's degradation for 10 days following transplantation.

An intravital laser-scanning microscope optimized for *in vivo* imaging (Olympus IV 100, Olympus, Center Valley, PA) was used with Olympus UplanFL objectives and Olympus FluoView IV10-ASW 1.2 software. Regions within the scaffold and the tissue were excited with a laser at 488 nm to outline the scaffold area. Regions of interest were analyzed using the FluoView FV300 software (V4.3, Olympus).

2.6. Scanning electron microscope (SEM) imaging

Hydrogel samples were placed on clean 1 cm aluminum SEM post (Ted Pella, Redding, CA). The samples were then air dried under a glass petri dish for a minimum of 6 h. After 6 h the samples were transferred to a SEM sample storage box, and placed in a vacuum desiccator overnight. After the samples were fully dehydrated they were permanently adhered to the SEM posts using high performance silver paste (Ted Pella, Redding, CA) to prevent the samples from coming loose in the microscope. The samples were then coated with a thin layer of AuPd using a Cressington 108 sputter coater (Ted Pella, Redding, CA) to improve conductivity. After preparation the samples were imaged in the Magellan 400 XHR SEM (FEI, Portland, OR) at 3 kV with a beam current of 25 pA. These operating conditions were chosen to minimize beam damage, while providing excellent topographical information about the hydrogel. Images were taken at several positions across the hydrogel samples at multiple magnifications to obtain information about the pore size distribution. As the hydrogel dehydrated it collapsed on itself. Areas of the hydrogel with pores collapsed further than the surrounding areas because there was less material present. This created topographical features at the surface of the dehydrated hydrogel that correspond to the pore size of the hydrated hydrogel allowing for the measurement of the pore size from the dehydrated samples.

Hydrogel samples were also imaged in EVO LS15 variable pressure SEM to obtain images of the hydrogel in its hydrated state. Samples were placed on peltier cooled stage and maintain just above the freezing point as the pressure was decreased to

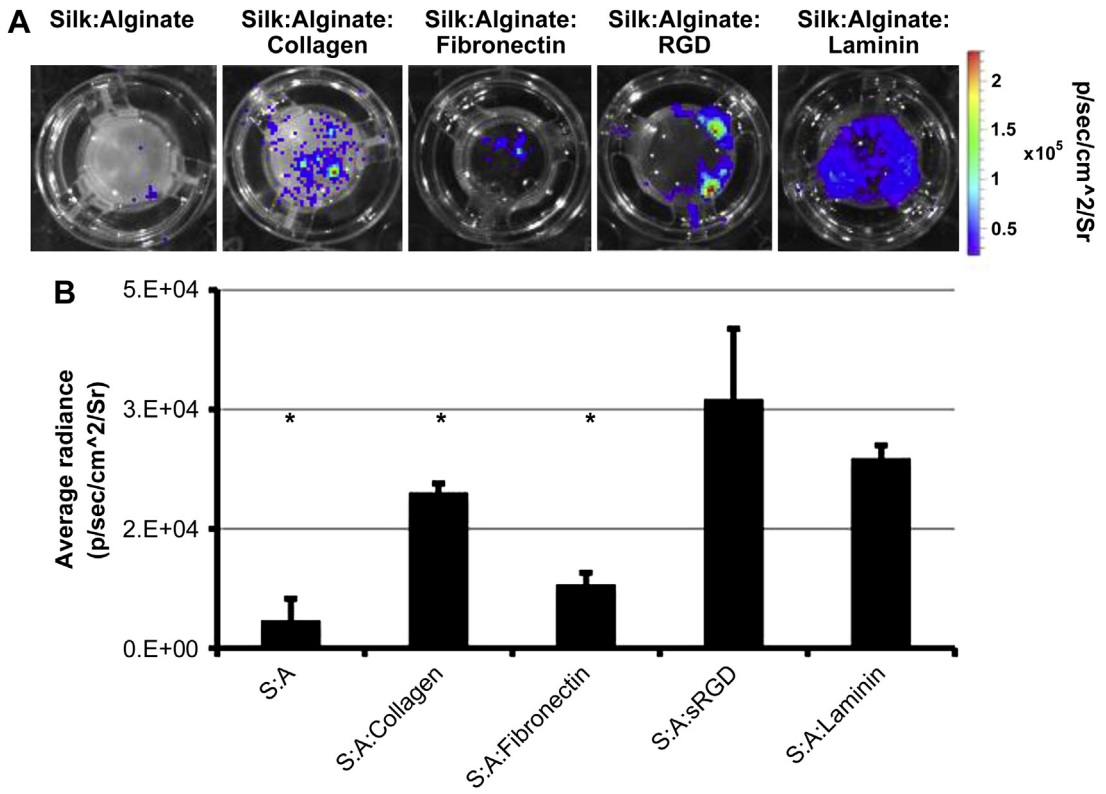

Fig. 1. Addition of ECM materials promotes cell adherence to the scaffold. D3 (mESC) stably expressing Fluc were plated on different scaffold composites and imaged 3 days after plating. A. Representative BLI images of the different scaffolds with D3 cells B. Quantification of BLI signal (*$p < 0.05$ unpaired 2 tails *T*test, $n = 3$).

prevent evaporation of the liquid. Samples were imaged at 25 kV using the back-scattered electron detector to image the hydrogel structure through the liquid.

2.7. Immune response assessment: histology and TNFα ELISA

The immune response was evaluated by histology and serology tests.

2.7.1. Histology

Scaffold (silk:alginate:laminin) was transplanted in the hind limb of 10 week old female BalbC mice ($n = 5$). A group of control mice went through a sham operation of the hind limb and were injected with 100 μl of PBS ($n = 5$). Two weeks after the transplantation, mice were sacrificed and skin samples and lymph nodes were retrieved. Tissue samples were stained with hematoxylin and eosin (H&E) stain and evaluated by a pathologist.

2.7.2. TNFα ELISA

BlabC mice were exposed to one of the following treatments: scaffold transplantation at the hind limb ($n = 4$), sham operation and subcutaneous PBS injection at the hind limb (negative control, $n = 3$) and intranasal exposure to E.Coli LPS (2.5 μl/mL, 20 μl/mouse, $n = 4$) (Sigma Aldrich). Blood was collected 3 h after treatment from all groups. The serum was extracted from the blood samples and analyzed using TNFa ELISA kit (Thermo Scientific, Rockford, IL).

2.8. In vivo cell survival

Rat mesenchymal stem cells (rMSCs) constitutively expressing Fluc, were cultured in rat marrow stromal cell growth medium (Cell Applications, San Diego, CA). 5×10^5 rMSC were trypsinized, pelleted, and resuspended in 100 μl of one of the following: PBS, growth factor reduced matrigel (BD biosciences, San Jose, CA), or a scaffold mixture (silk:alginate:laminin) solid and liquid. The cells were transplanted in the hind limb of the mouse (10 week old female nude mice, Nu/Nu; Charles River, $n = 5$ per group). BLI was done 1, 4, 7, 14, 21, 28 and 35 days following transplantation. D-Luciferin (3 mg/mouse) diluted in PBS (100 μL total volume) was injected IP. Mice were imaged for 40 min following luciferin administration using IVIS-200 equipped with a charge-coupled device camera (Caliper). Imaging was performed using open filters with alternating acquisition times (1 min and 30 s). Regions of interest were drawn over the mice site of transplantation using the images of the acquisition times with the highest signal in each group. All data was analyzed using Living Image software (V4.2, Caliper Life Sciences).

2.9. Rheology

Hydrogel properties were determined by oscillatory rheology. Rheological experiments were performed with an Anton Paar rheometer, equipped with peltier temperature control (set to 37 °C, Physica MCR301 R, Julabo AWC 100), in conjunction with a stainless steel probe (8 mm diameter; flat, PP08). To prevent slipping and, in accordance with the manufacturer, waterproof sandpaper (400-grit, 3 M) was attached to both the probe and bottom plate using double adhesive tape (3 M). A humid chamber was achieved by filling distilled water into the rim around platform and placing a chamber cover on top. For strain amplitude sweep experiments, the probe was lowered until a normal force of 0.02 N was reached to prevent slipping. Experiments were performed over an amplitude range of 0.25–50% with an angular frequency of 10 s^{-1}. The recorded storage (G') and loss (G'') moduli were converted into the complex modulus G

$$G = G' + iG'' \tag{1}$$

Young's modulus E was calculated according to

$$E = 2G(1 + \nu) \tag{2}$$

with a Poisson's ratio υ of 0.5 (i.e., volume is conserved since the gel mainly consists of water), as reported for hydrogels. Data were analyzed using the Rheoplus software (V3.21, Anton Paar) and Excel (Office 2010).

2.10. Tuning the elasticity of the scaffold

The ability to tune the scaffold's elasticity *in-vitro* was measured using 3 conditions: a) varying the ratio of silk to alginate, b) incubation of scaffolds (S3:A2) in 95% FBS and 95% FBS supplemented with 25 mM $CaCl_2$ for 20–360 min and c) incubation of the scaffold in alternating conditions: 30 min in FBS, 30 min in FBS supplemented with 25 mM $CaCl_2$, for up to 150 min.

2.11. Statistical analysis

Cell culture experiments were analyzed using the Student's *t*-test (two-sided, paired). Mice experimental analysis was done using a one way ANOVA followed by Tukey's post hoc multiple comparison test. Values of $p < 0.05$ were considered statistically significant.

3. Results

3.1. Cell adherence to the silk:alginate biocomposite

One of the criteria for a successful scaffold is the ability for cells to adhere to it. To overcome the silk:alginate biocomposite's (referred to as the hydrogel) inability to facilitate cell adherence (Fig. 1A), we introduced different ECM materials into the hydrogel. The hydrogel was supplemented with one of the following: Collagen I, fibronectin, cyclic RGD or laminin. After gelation we plated mESCs constitutively expressing of Fluc on the hydrogel. 72 h after plating, cells were washed and imaged using BLI. The bioluminescence signal (BL signal) corresponded to the presence of adhered cells (Fig. 1A). Addition of collagen I, fibronection, or cyclic RGD to the hydrogel enhanced the adherence of cells. However, the pattern of the cell growth was sparse and didn't cover the entire scaffold. Addition of laminin induced a continuous pattern of cell growth, as reflected by the strong BL signal (Fig. 1A). Although there was no significant difference in BL signal between the RGD group and the laminin group (Fig. 1B), we chose to continue our experiments with silk:-alginate:laminin mixture since it induced a homogenous and continues growth pattern which is the desired growth pattern.

3.2. Intravital and scanning electron microscopy

We examined the scaffold's biodegradability *in-vitro* using E-SEM and *in-vivo* using IVM. The pore size of fresh scaffolds and scaffolds after 7 days of incubation in media was evaluated using both environmental and traditional SEM (Fig. 2A). Analysis of the pore size was done using the evaporated sample in traditional SEM. In the fresh scaffold 86% of the pores had an averaged size under 1 μm. Pore size is an important characteristic of the scaffold it dictates the diffusion of substrates and the layout of the cells. The silk:alginate scaffold has small pore size therefore it gives good support to the transplanted cells, while allowing nutrients diffusion to occur. After 7 days of incubation, the pore size was smaller.

In order to follow the degradation of the scaffold *in vivo* using IVM, alginate labeled with RBITC (alginate–RBITC) was used for the hydrogel mix. The fluorescent hydrogels were transplanted in mice in dorsal window chambers and followed for 10 days using IVM (Fig. 2B). Region of interest analysis of the hydrogel fluorescence revealed a significant decrease in the fluorescent signal on day 10, which corresponds to degradation of the alginate (Fig. 2C).

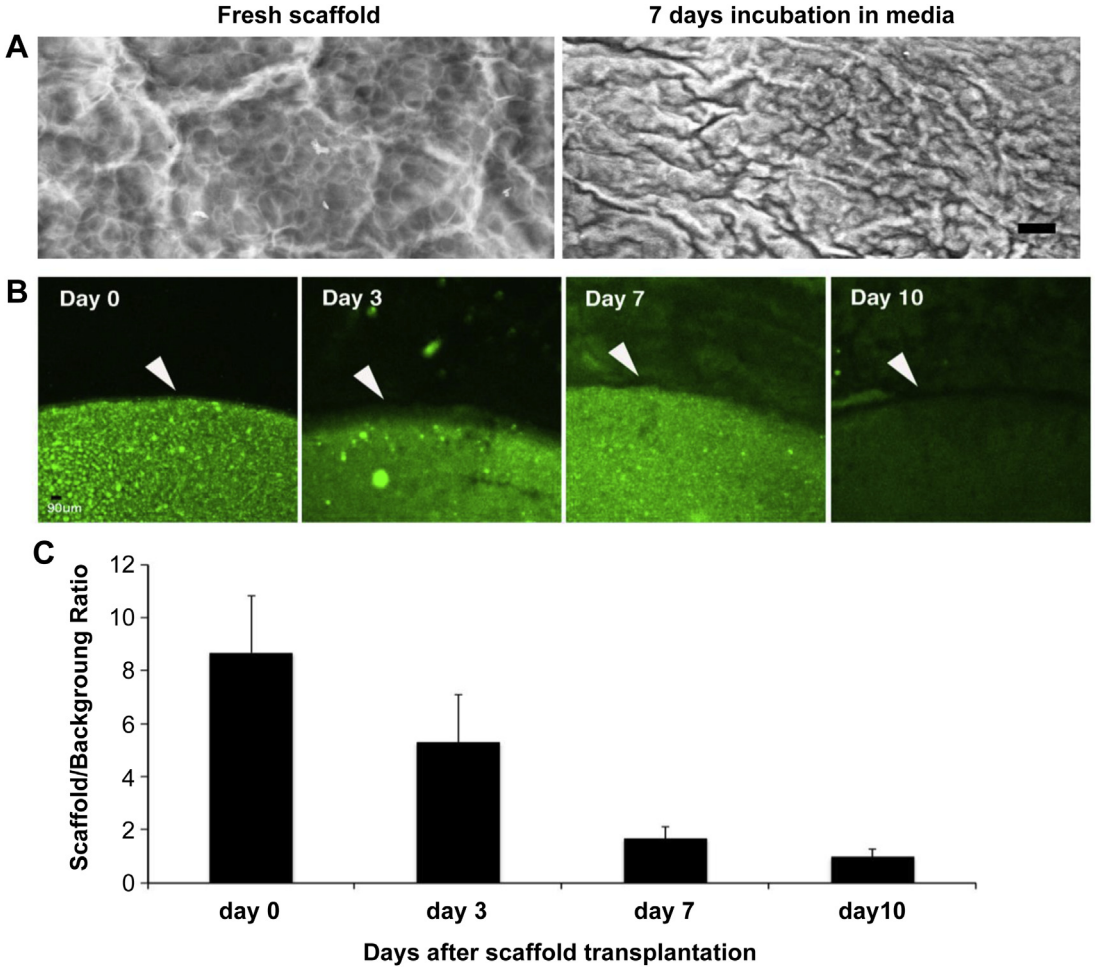

Fig. 2. Scaffold structural changes following incubation in media and transplantation in a mouse. Scaffold samples pore size was evaluated using E-SEM (scale bar 20 μm) B. Scaffolds labeled with FITC were transplanted in BalbC mice using the window chamber model. Scaffold fluorescence was evaluated using IVM. C. Quantification of fluorescent signal, scaffold to background ratio.

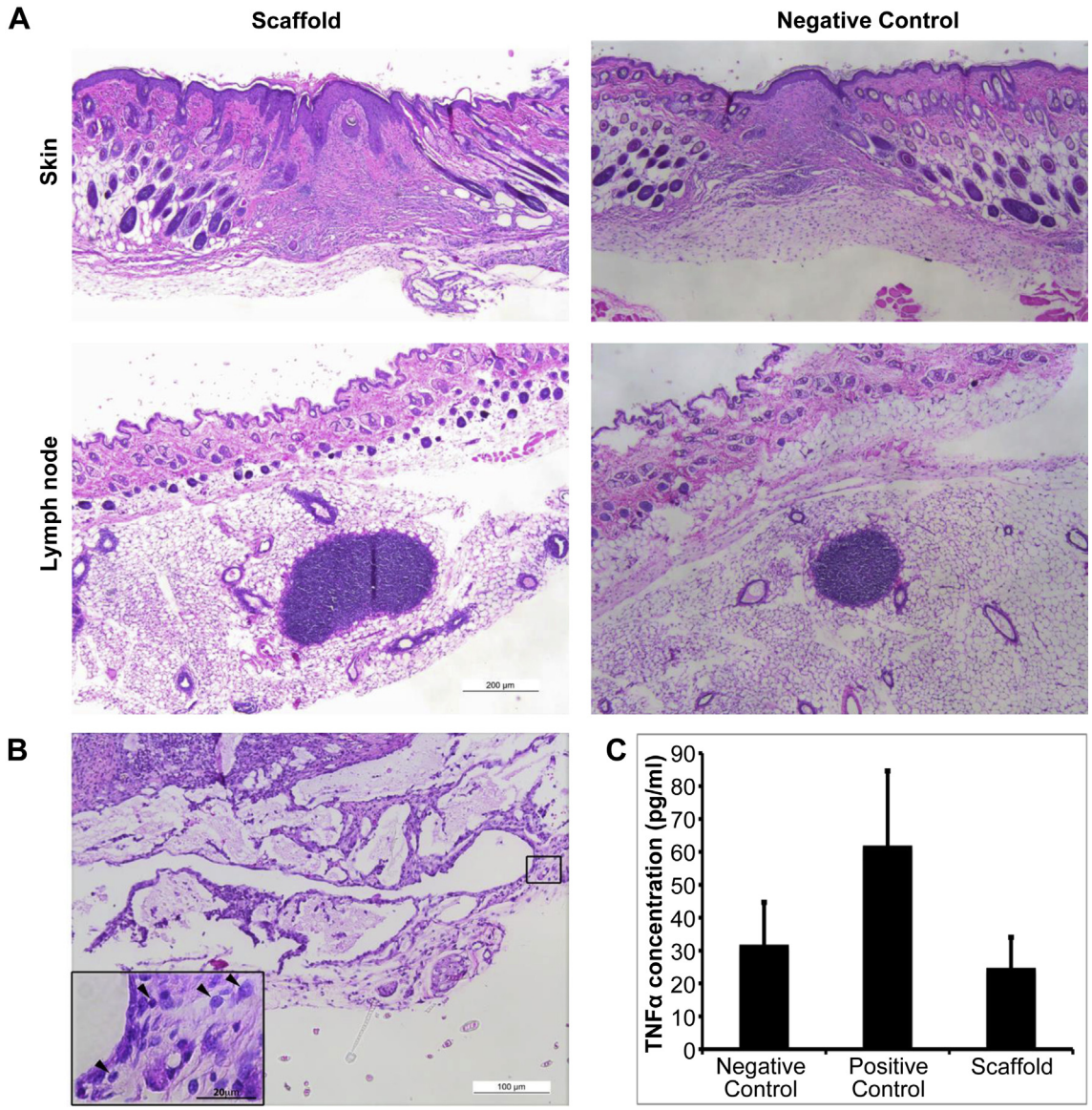

Fig. 3. The silk:alginate:laminin scaffold induces a very mild immune response. Mice were treated with PBS injection (negative control $n = 5$), LPS intra-nasal exposure (positive control $n = 4$), and transplanted with the scaffold ($n = 4$). Mice were sacrificed, blood and tissue samples were taken for histology evaluation and TNFα analysis. A. representative images of skin wound healing and regional lymph node following treatment. There was no significant difference in wound healing response or lymph node size due to scaffold transplantation. B. Histology section of the scaffold area, mild immune reaction was observed. Inset in B shows higher magnification: small numbers of reactive macrophages and multinucleated giant cells (arrows), small amounts of fibroplasia. C. Serum samples were analyzed for TNFα. The scaffold did not induce an elevation in TNFα levels.

3.3. Scaffold induced immune response test

The immune response plays a pivotal role in regenerative medicine. Cell survival following transplantation is often compromised by immune response. Hence it is of the utmost importance the scaffold will not induce an additional response. We examined the acute, as well as the chronic immune reaction to the scaffold. Scaffolds were transplanted in the hind limb of BalbC mice. 12 days after transplantation the mice were sacrificed and the tissue surrounding the scaffold was retrieved and evaluated histologically. There was no difference in skin healing pattern between the scaffold group and the sham-operation group. Skin and lymph node sections revealed an appropriate 12-day wound healing response, which included maturing granulation tissue, minimal neutrophils, some macrophages and lymphocytes, as well as re-epithelization of the epidermis (Fig. 3A). Lymph nodes showed mild reactive hyperplasia (Fig. 3A). At the scaffold transplantation site few reactive macrophages and multinucleated giant cells were observed, and a small amount of fibroplasia was seen (Fig. 3B).

The immune reaction induction was also evaluated through TNFα levels in the serum. TNFα is involved in systemic inflammation and is one of the key cytokines that stimulates the acute phase immune reaction. TNFα levels were measured 3 h following transplantation of the scaffold. The ELISA test revealed there was no significant difference between the negative control group and the scaffold group, while TNF levels in the positive control group, which was exposed to intranasal E.Coli LPS were significantly elevated ($p < 0.05$, unpaired *T*test) (Fig. 3C).

3.4. Stem cell survival using the silk:alginate:laminin scaffold

The survival of stem cells following transplantation is dependent on the immune response, as well as on the microenvironment

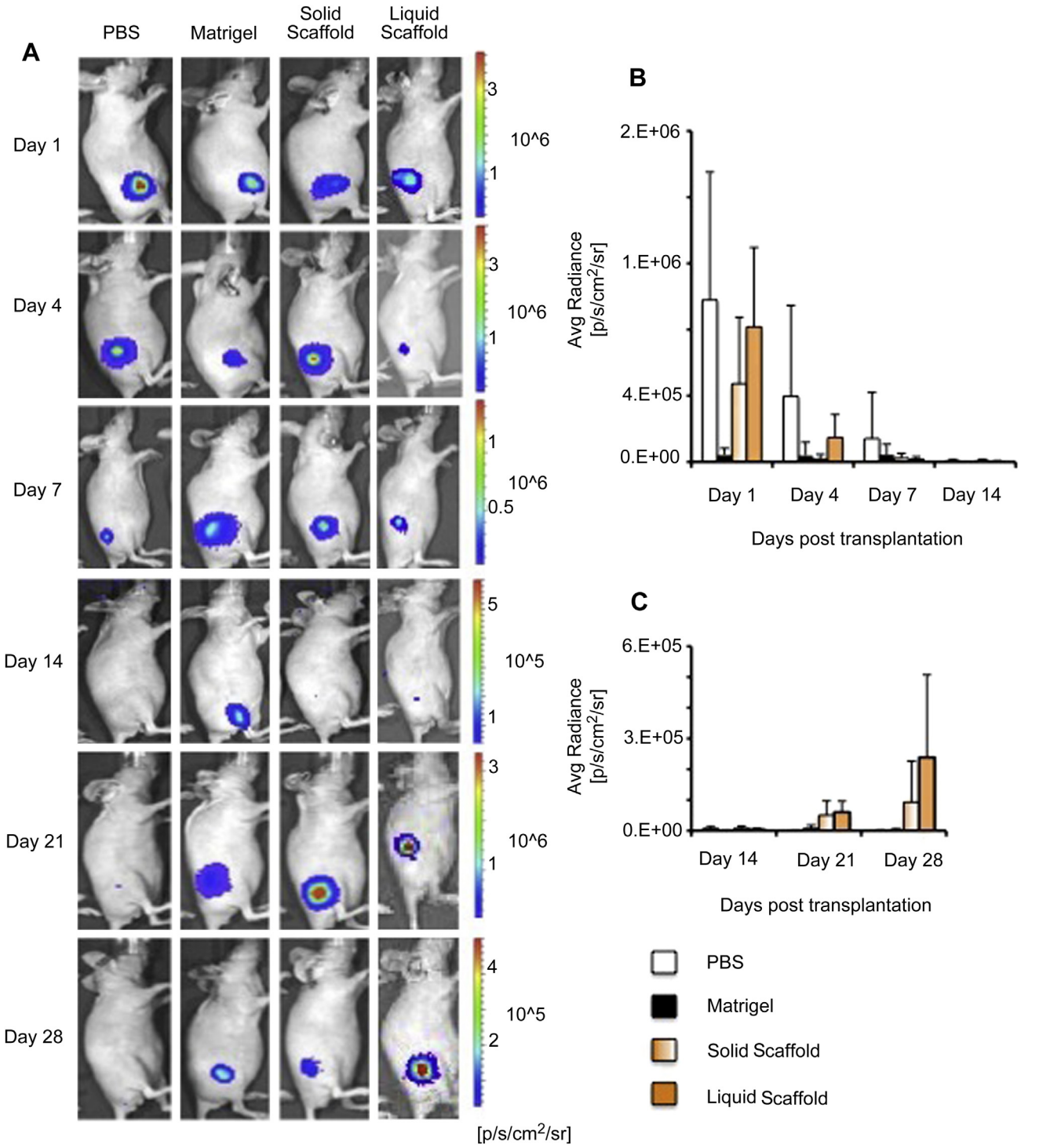

Fig. 4. *In vivo* survival of rMSC. rMSC stably expressing Fluc were transplanted in nude mice hind limb with PBS, matrigel and scaffold. A. BLI images of representative mice at days 1, 4 7, 14, 21 and 28 post transplantation. B & C. Quantification of BLI signal ($^*p < 0.05$ unpaired 2 tails *T*test, $n = 5$ per group).

of the cells. In recent years matrigel has become the leading scaffold for stem cell transplantation in animal experiments. However, implementing matrigel in the clinical arena is impossible due to its means of production, and the variability between different batches. In order to assess the contribution of the silk:alginate:laminin scaffold to stem cell survival, we transplanted rMSC stably expressing Fluc in nude mice with one of the following: PBS, growth factor reduced matrigel, or the silk:alginate:laminin scaffold (solid and liquid). rMSC survival was followed for 35 days following transplantation using BLI (Fig. 4A). The BL signal in all groups decreased over the first two weeks after transplantation, indicating that rMSC survival in all groups was poor. However, on day 21 there was a significant elevation in BL signal at the matrigel and scaffold groups, while PBS group showed a continuing reduction in BL signal throughout the measurement period. The phenomenon of transplanted stem cells recovery on day 21 was also reported by Perin et al., who used matrigel for stem cell transplantation [25].

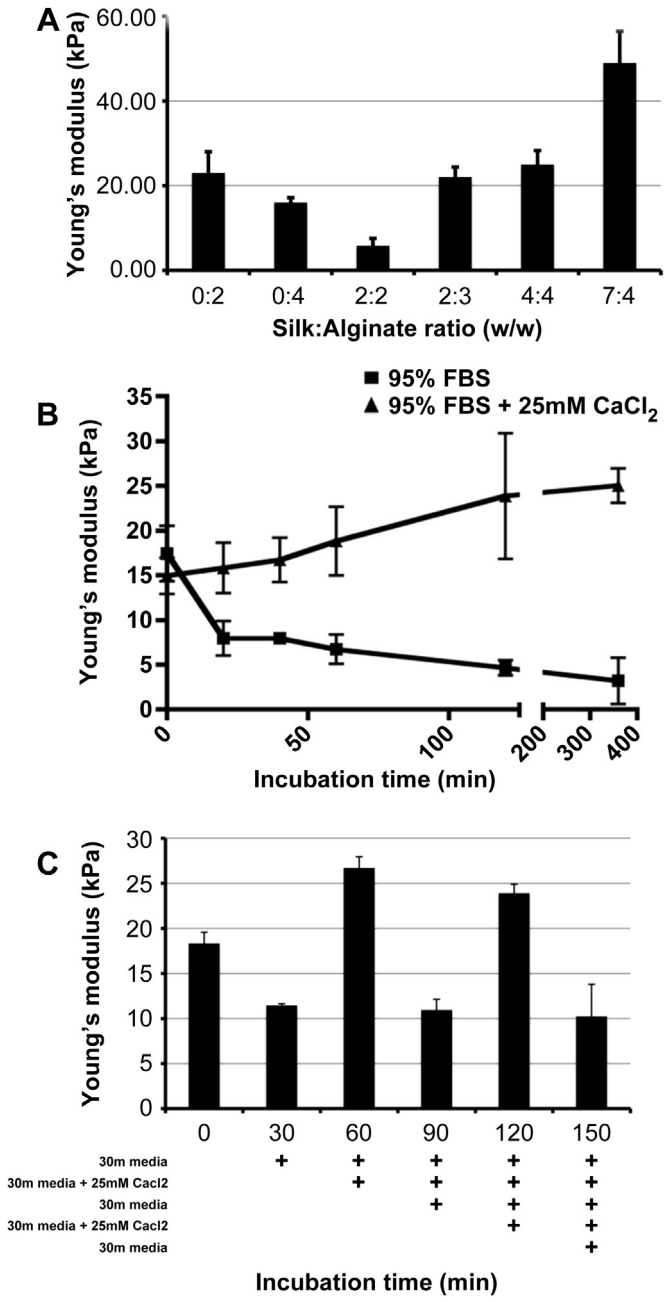

Fig. 5. Tuning the elasticity of the scaffold. The scaffold's elasticity was measured using a rheometer. The elasticity values are varying under different conditions. A. Variation of the silk:alginate ratio allows tuning of the scaffold's elasticity. B. Incubation of scaffolds (S3:A2) in 95% FBS and 95% FBS supplemented with 25 mM $CaCl_2$ for 20–360 min. C. The scaffold's elasticity is tunable when it was incubated in alternating conditions (S3:A2).

On day 28, the BL signal in the PBS group was reduced to a level equal to the background level and the matrigel group displayed a slight elevation in signal, whereas a steady high BL signal was observed in the scaffold groups (Fig. 4B, C). Thus, the results demonstrate a significantly superior performance of the scaffold in maintaining cell survival compared to matrigel.

3.5. Tuning of the scaffold elasticity

The mechanical properties of the microenvironment, such as elasticity, play a pivotal role in stem cell differentiation [9]. The ability to culture stem cells with certain elasticity can increase the yield of any particular differentiation path. We found that in our scaffolds, elasticity is highly dependent on the silk to alginate ratio (Fig. 5A). This enables us to precisely target different elasticity moduli when casting the hydrogel, resulting in a scaffold that can be used for several differentiation pathways. Typically, once cast, scaffolds have a constant elasticity, and it is unfeasible to change this. Here, we predicted that by varying the concentration of crosslinking ions in the cell media, it would be possible for us to tune the elasticity in vitro (Fig. 5C). We managed to achieve fine tuning of the elasticity through incubation of the scaffolds under alternating conditions with and without the crosslinker, which resulted in an increase and decrease in elasticity, i.e. the change in elasticity is reversible (Fig. 5C).

Furthermore, during cell culture, scaffold's elasticity was altered due to the presence of degrading proteins found in the media and by cellular secretions. This leads to an increase in elasticity over time. However, the addition of crosslinker ($CaCl_2$) to the media prevents this alteration (Fig. 5B). The ability to control the scaffold's elasticity *in-vitro* has the potential to facilitate desired differentiation paths.

4. Discussion

The combination of silk and alginate, results in a hybrid class of rapidly gelling, physically stable hydrogels that is promising for many applications in regenerative and pharmaceutical medicine. Alginate, composed of blocks of the polysaccharides D-mannuronic (M) and L-guluronic (G) acid residues, can rapidly form stable hydrogels in the presence of divalent ions such as magnesium, calcium, strontium or barium [26,27]. Gel formation is caused by chelation of ions by D-guluronic acid. Mechanical and physical properties of alginate hydrogels can be fine-tuned as needed for specific applications by the use of alginates of different average molecular weights, by the variation of the ratio of the M- and G-blocks, and/or the ion concentration used for crosslinking. However, alginate gels will quickly dissolve in the absence of divalent ions, or in the presence of acids or other ions (e.g. phosphate), subsequently limiting their usefulness for long-term applications. On the other hand, silk fibroin, a macromolecular protein derived from silk worms (e.g., *B. mori*), can also be made into gels by various means, and remains stable over long periods of time when physically crosslinked by partial or complete dehydration [28]. However, in strong contrast to alginate, the silk fibroin crosslinking process is time-consuming, and mostly results in an insoluble aggregation [29]. Furthermore, silk fibroin offers only a very limited range by which its mechanical and physical properties are controllable, if at all (depending on the specific silk protein amino acid sequence).

The reported silk–alginate hybrid gels benefit from a synergy of the traits of the two materials: it has biocompatibility characteristics, has tunable mechanical and morphological properties, can be crosslinked very quickly, thereby leading to increased physical.

However, although the silk–alginate hydrogel possess desired properties, it was failing as a scaffold for cell culture due to lack of cell adherence, which is one of the basic requirements of a scaffold. A variety of ECM materials were examined as a supplement in order to overcome this problem. Ultimately, the addition of laminin achieved the best cell growth *in-vitro*. The hydrogel was tested for cell adherence using embryonic stem cells (ESC), which are known to be very challenging to culture. While the ESCs didn't grow on the silk–alginate hydrogel as was manifested by the lack of BL signal in culture, the addition of laminin to the hydrogel yielded a very strong BL signal which indicated of the growth of ESCs. The hydrogel was also tested *in-vivo* using mesenchymal stem cells and outperformed matrigel as a solid scaffold, and as a liquid mixture.

Current limitations of this system include the lack of *in vivo* gelation, which is a desirable property for a hydrogel, due to absence of a sufficient concentration of bivalent ions in the body. Furthermore, the presented gelation process currently does not enable us to create anisotropic hydrogel, i.e. gels with a stiffness or ECM molecule gradient. Therefore future studies will include improvement of the gelation platform to enable formation of anisotropic hydrogel and the option of *in-vivo* gelation.

5. Conclusions

The success of stem cell therapy is dependent on the transplanted stem cells as well as on the stem cell environment. Our results show that by mimicking the stem cell microenvironment more closely, through the alginate–silk–laminin hydrogel we are capable of improving the survival viable stem cells, paving the way for more efficient regenerative medicine therapies.

Acknowledgments

Keren Ziv is a Pfizer fellow of the Life Science Research Foundation. The silk was kindly provided by Rucsanda Carmen Preda from David L. Kaplan's Laboratory, Tufts University. Boston, MA. The SEM images were taken using EVO LS15 VPSEM with Extended Pressure Technology with the kind help of Stephen W. Joens, applications Specialist from Carl Zeiss Microscopy, LLC. Thornwood, NY. Laura Sarah Sasportasis supported by a Fulbright Science and Technology Fellowship, a Stanford Weiland Fellowship, a Student Fellowship from the Society for Nuclear Medicine (SNM), and an International Student Fellowship from the Howard Hughes Medical Institute (HHMI). SEM analysis by Paul Kempen was funded through the NIH NCI Center for Cancer Nanotechnology Excellence Grants CCNE U54 CA119367 (S.S.G.), CCNE U54 U54CA151459 (SSG). The imaging studies were done at the Stanford Center for Innovation in In-Vivo Imaging (SCI3).

References

[1] Berthiaume F, Maguire TJ, Yarmush ML. Tissue engineering and regenerative medicine: history, progress, and challenges. Annu Rev Chem Biomol Eng 2011;2:403–30.
[2] Chun YS, Byun K, Lee B. Induced pluripotent stem cells and personalized medicine: current progress and future perspectives. Anat Cell Biol 2011;44(4):245–55.
[3] Iglesias-Garcia O, Pelacho B, Prosper F. Induced pluripotent stem cells as a new strategy for cardiac regeneration and disease modeling. J Mol Cell Cardiol 2013;62:43–50.
[4] Sacco A, Doyonnas R, Kraft P, Vitorovic S, Blau HM. Self-renewal and expansion of single transplanted muscle stem cells. Nature 2008;456:502–6.
[5] Krishnamurthy NV, Gimi B. Encapsulated cell grafts to treat cellular deficiencies and dysfunction. Crit Rev Biomed Eng 2011;39(6):473–91.
[6] Morrison SJ, Spradling AC. Stem cells and niches: mechanisms that promote stem cell maintenance throughout life. Cell 2008;132:598–611.
[7] Fuchs E, Tumbar T, Guasch G. Socializing with the neighbors: stem cells and their niche. Cell 2004;116:769–78.
[8] Hines M, Nielsen L, Cooper-White J. The hematopoietic stem cell niche: what are we trying to replicate? J Chem Technol Biotechnol 2008;83:421–43.
[9] Gilbert PM, Havenstrite KL, Magnusson KE, Sacco A, Leonardi NA, Kraft P, et al. Substrate elasticity regulates skeletal muscle stem cell self-renewal in culture. Science 2010;329:1078–81.
[10] Montarras D, Morgan J, Collins C, Relaix F, Zaffran S, Cumano A, et al. Direct isolation of satellite cells for skeletal muscle regeneration. Science 2005;309:2064–7.
[11] Furth ME, Atala A, Van Dyke ME. Smart biomaterials design for tissue engineering and regenerative medicine. Biomaterials 2007;28:5068–73.
[12] Celebi B, Cloutier M, Rabelo RB, Mantovani D, Bandiera A. Human elastin-based recombinant biopolymers improve mesenchymal stem cell differentiation. Macromol Biosci 2012;12(11):1546–54.
[13] Williams D. Collagen: ubiquitous in nature, multifunctional in devices. Med Device Technol 1998;9(6):10–3.
[14] Dawson E, Mapili G, Erickson K, Taqvi S, Roy K. Biomaterials for stem cell differentiation. Adv Drug Deliv Rev 2008;60:215–28.
[15] Boonen KJ, Post MJ. The muscle stem cell niche: regulation of satellite cells during regeneration. Tissue Eng Part B Rev 2008;14:419–31.
[16] Dengler J, Song H, Thavandiran N, Masse S, Wood GA, Nanthakumar K, et al. Engineered heart tissue enables study of residual undifferentiated embryonic stem cell activity in a cardiac environment. Biotechnol Bioeng 2011;108:704–19.
[17] Kreutziger KL, Murry CE. Engineered human cardiac tissue. Pediatr Cardiol 2011;32:334–41.
[18] Oliveira MB, Mano JF. Polymer-based microparticles in tissue engineering and regenerative medicine. Biotechnol Prog 2011;27(4):897–912.
[19] Singelyn JM, Christman KL. Injectable materials for the treatment of myocardial infarction and heart failure: the promise of decellularized matrices. J Cardiovasc Transl Res 2010;3(5):478–86.
[20] Williams DF. On the nature of biomaterials. Biomaterials 2009;30:5897–909.
[21] Levenberg S, Rouwkema J, Macdonald M, Garfein ES, Kohane DS, Darland DC, et al. Engineering vascularized skeletal muscle tissue. Nat Biotechnol 2005;23(7):879–84.
[22] Leong MF, Toh JK, Du C, Narayanan K, Lu HF, Lim TC, et al. Patterned prevascularised tissue constructs by assembly of polyelectrolyte hydrogel fibres. Nat Commun 2013;4:2353.
[23] Brown E, Munn LL, Fukumura D, Jain RK. In vivo imaging of tumors. Cold Spring Harb Protoc July 1 2010;2010(7). pdb.prot5452.
[24] Mladenovska K, Cruaud O, Richomme P, Belamie E, Raicki RS, Venier-Julienne MC, et al. 5-ASA loaded chitosan-Ca-alginate microparticles: preparation and physicochemical characterization. Int J Pharm 2007;345(1–2):59–69.
[25] Perin EC, Tian M, Marini 3rd FC, Silva GV, Zheng Y, Baimbridge F, et al. Imaging long-term fate of intramyocardially implanted mesenchymal stem cells in a porcine myocardial infarction model. PLoS One 2011;6(9):e22949.
[26] Pathak TS, Yun JH, Lee J, Paeng KJ. Effect of calcium ion (cross-linker) concentration on porosity, surface morphology and thermal behavior of calcium alginates prepared from algae (Undaria pinnatifida). Carbohydr Polym 2010;81:633–9.
[27] Zimmermann H, Wahlisch F, Baier C, Westhoff M, Reuss R, Zimmermann D, et al. Physical and biological properties of barium cross-linked alginate membranes. Biomaterials 2007;28(7):1327–45.
[28] Vepari C, Kaplan DL. Silk as a biomaterial. Prog Polym Sci 2007;32(8–9):991–1007.
[29] Lu S, Wang X, Lu Q, Zhang X, Kluge JA, Uppal N, et al. Insoluble and flexible silk films containing glycerol. Biomacromolecules 2010;11(1):143–50.